

Equivalence Principle and Bound Kinetic Energy

Michael A. Hohensee* and Holger Müller

Department of Physics, University of California, Berkeley 94720, USA

R. B. Wiringa

Physics Division, Argonne National Laboratory, Argonne, Illinois 60439, USA

(Dated: February 26, 2022)

We consider the role of the internal kinetic energy of bound systems of matter in tests of the Einstein equivalence principle. Using the gravitational sector of the standard model extension, we show that stringent limits on equivalence principle violations in antimatter can be indirectly obtained from tests using bound systems of normal matter. We estimate the bound kinetic energy of nucleons in a range of light atomic species using Green's function Monte Carlo calculations, and for heavier species using a Woods-Saxon model. We survey the sensitivities of existing and planned experimental tests of the equivalence principle, and report new constraints at the level of between a few parts in 10^6 and parts in 10^8 on violations of the equivalence principle for matter and antimatter.

General relativity follows from the Einstein equivalence principle (EEP), which holds that in any local Lorentz frame about any point in spacetime, the laws of physics are described by the standard model of particle physics and special relativity [1]. Both general relativity and the standard model are believed to be the low energy limits of some as yet unknown complete theory of physics at high energy scales. Such a theory might generate violations of EEP at experimentally accessible energy scales [2–4], although its exact form is unknown. Thus it is important to search for EEP violation in as many different places as possible. We use the Standard Model Extension (SME) [4], a flexible and widely applied [5] framework for describing violations of EEP. The SME is an effective field theory that phenomenologically augments the Standard Model action with terms that break local Lorentz invariance and other tenets of EEP [6], while preserving energy conservation, gauge invariance, and general covariance. As in other models [2], EEP-violation in the SME can manifest in multiple ways. In particular, it may be strongly suppressed in normal matter relative to antimatter [6, 7]. Although the equivalence principle has been validated with extremely high precision for normal matter [8], the situation for antimatter is less clear.

In this Letter, we show that in the SME, EEP violation in antimatter can be constrained by tests using bound systems of normal matter. We clearly demonstrate how an anomaly that violates the weak equivalence principle for free particles generates anomalous gravitational redshifts in the energy of systems in which they are bound, in proportion to the systems' internal kinetic energy. Using a nuclear shell model, we estimate the sensitivity of a variety of atomic nuclei to EEP violation for matter and antimatter, and illustrate points of commonality between older representations of EEP violation based on neutron excess and baryon number, and that of the SME. We show that existing experimental [8–17] limits on spin-independent EEP violation in matter and antimatter [7] are up to ten times tighter than previously thought, and

could be made tighter still, provided more precise estimates of the bound kinetic energy of particles in atomic systems. We focus on EEP-violation in conventional matter (made up of protons, neutrons, and electrons), and as in prior work [5–7], assume that anomalies affecting force-carrying virtual particles are negligible. Using general covariance, we define our coordinates such that photons follow null geodesics, ensuring that electromagnetic fields do not violate EEP.

In the SME, spin-independent violations of EEP acting on a test particle of mass m^w are described in its action [6]

$$S = - \int m^w c \sqrt{-(g_{\mu\nu} + 2(\bar{c}^w)_{\mu\nu}) dx^\mu dx^\nu} + (a_{\text{eff}}^w)_\mu dx^\mu, \quad (1)$$

where the superscript $w = p, n, \text{ or } e$ (for proton, neutron, or electron) indicates the type of particle in question, $g_{\mu\nu}$ is the metric tensor, dx^μ is the interval between two points in spacetime, and c is the speed of light. The $(\bar{c}^w)_{\mu\nu}$ tensor describes a fixed background field that modifies the effective metric that the particle experiences, and thus its inertial mass relative to its gravitational mass. The four-vector $(a_{\text{eff}}^w)_\mu = \{(1 - U\alpha)(\bar{a}_{\text{eff}}^w)_0, (\bar{a}_{\text{eff}}^w)_j\}$, where U is the Newtonian potential, represents the particle's coupling to a field with a non-metric interaction with gravity. As $(a_{\text{eff}}^w)_\mu$ is CPT-odd [4], this term enters with opposite sign in the action for an antiparticle \bar{w} . Both $(\bar{c}^w)_{\mu\nu}$ and $(a_{\text{eff}}^w)_\mu$ vanish if general relativity is valid. For convenience, Eq. (1) includes an unobservable scaling of the particle mass by $(1 + \frac{5}{3}(\bar{c}^w)_{00})$.

We focus on the isotropic subset of this model [6], in which $(\bar{c}^w)_{\mu\nu}$ is diagonal and traceless, and the spatial terms in the vector $(a_{\text{eff}}^w)_\mu$ vanish. In this limit, EEP-violation is described by the comparatively poorly constrained $(\bar{c}^w)_{00}$ coefficients [5], and the $(\bar{a}_{\text{eff}}^w)_0$ terms, which cannot be measured in non-gravitational experiments [4]. In the non-relativistic, Newtonian limit, less the rest mass energy and assuming that any violations of EEP must be small, the single particle Hamiltonian

produced by the action (1) is given by

$$H = \frac{1}{2} m^w v^2 - m_g^w U, \quad (2)$$

where the effective gravitational mass m_g^w is given by

$$m_g^w = m^w \left(1 - \frac{2}{3} (\bar{c}^w)_{00} + \frac{2\alpha}{m^w} (\bar{a}_{\text{eff}}^w)_0 \right).$$

Experimentally observable EEP violations are proportional to the particle's gravitational to inertial mass ratio

$$\frac{m_g^w}{m^w} = 1 - \frac{2}{3} (\bar{c}^w)_{00} + \frac{2\alpha}{m^w} (\bar{a}_{\text{eff}}^w)_0 \equiv 1 + \beta^w, \quad (3)$$

and are described here, as elsewhere [7, 9, 18], by the parameter β^w . From Eq. (3), we see that both $(\bar{c}^w)_{00}$ and $(\bar{a}_{\text{eff}}^w)_0$ are responsible for violations of the weak equivalence principle, an aspect of EEP [19], since they produce particle-dependent rescalings of the effective gravitational potential. In addition, EEP violation is not apparent in the non-relativistic motion of a free particle if $\alpha(\bar{a}_{\text{eff}}^w)_0 = (m^w/3)(\bar{c}^w)_{00}$, although it remains manifest in the motion of the antiparticle \bar{w} , for which $\beta^{\bar{w}} = -2\alpha/m^w(\bar{a}_{\text{eff}}^w)_0 - 2/3(\bar{c}^w)_{00}$ [6]. As we now demonstrate, however, the antimatter anomaly $\beta^{\bar{w}}$ does contribute to tests involving non-gravitationally bound systems of matter, thanks to the anomalous gravitational redshift produced by $(\bar{c}^w)_{00}$ in the energies of bound systems.

For a bound system of particles, the total Hamiltonian is a sum of single-particle Hamiltonians, plus an interaction energy V_{int} that is assumed to be free of EEP-violating terms. As implicit in Eq. (2), we take the system's squared center of mass velocity \bar{v}^2 to be small, and of similar order as the relevant change ΔU it explores in the gravitational potential. Since the system is non-gravitationally bound, however, we cannot assume that the same is true of its constituent particles. Thus we must include terms proportional to $v_{w,j}^2 U/c^2$ in our Hamiltonian, where $v_{w,j}$ is the instantaneous velocity of the j th bound particle of species w . In the limit that $\bar{v} \ll v_{w,j} \ll c$, we may approximate $v_{w,j}^2 = (\bar{v} + \delta v_{w,j})^2 \approx \bar{v}^2 + (\delta v_{w,j})^2$, (dropping the mixed $\bar{v}(\delta v_{w,j})$ terms which make little contribution to the bound kinetic energy) and obtain

$$H = V_{\text{int}} + \sum_w \left[\frac{1}{2} m^w N^w \bar{v}^2 - m^w N^w U (1 + \beta^w) + \frac{1}{2} \sum_{j=1}^{N^w} (\delta v_{w,j})^2 \left(1 + \frac{3U}{c^2} + \frac{2U}{3c^2} (\bar{c}^w)_{00} \right) \right]. \quad (4)$$

The second line in Eq. (4) represents the system's internally bound kinetic energy T_{int} , and includes a term that contributes to the system's conventional gravitational redshift, as well as a term proportional to $(\bar{c}^w)_{00}$ and the

gravitational potential U . This last term corresponds to an anomalous gravitational redshift of the bound state energies. To evaluate this term for bound quantum states, we recast it in terms of the momenta $\delta \vec{p}_{w,j}$ conjugate to the particle displacements $\delta x_{w,j} = x_{w,j} - \bar{x}$ from the system's center of mass \bar{x} . The momenta satisfy $\delta \vec{p}_{w,j} = \partial H / \partial (\delta \vec{v}_{w,j})$, and so

$$(\delta \vec{p}_{w,j}) = m^w (\delta \vec{v}_{w,j}) \left(1 + \frac{3U}{c^2} + \frac{2U}{3c^2} (\bar{c}^w)_{00} \right). \quad (5)$$

The bound kinetic energy T_{int} in Eq. (4) is thus

$$T_{\text{int}} = \sum_w \sum_{j=1}^{N^w} \frac{(\delta p_{w,j})^2}{2m^w} \left(1 - \frac{3U}{c^2} - \frac{2U}{3c^2} (\bar{c}^w)_{00} \right). \quad (6)$$

Note that in general, to ensure that the system's mass defect is subject to a conventional gravitational redshift in the absence of EEP-violation, V_{int} must depend upon U . If EEP is satisfied, the variation of the mass defect $m'_A = (V_{\text{int}} + T_{\text{int}})/c^2$ for a system A in a gravitational potential U is such that the ratio $m'_A(U_1)/m'_A(U_2) = 1 + (U_1 - U_2)/c^2$. Due to our initial scaling of the particle mass in Eq. (1), the factor in parenthesis in Eq. (6) contains terms proportional to 1, U , $U(\bar{c}^w)_{00}$, but not $(\bar{c}^w)_{00}$ alone. This, along with our assumption that V_{int} is independent of $(\bar{c}^w)_{00}$ and $(\bar{a}_{\text{eff}}^w)_0$, implies that the ratio $m'_A(U_1)/m'_A(U_2)$ does not generate additional cross terms in $U(\bar{c}^w)_{00}$, and we can therefore write the total Hamiltonian for a bound system A as

$$H = \frac{1}{2} M_A \bar{v}^2 - M_A U \left(1 + \beta^A + \frac{2}{3} \sum_w \frac{T_{\text{int}}^w}{M_A c^2} (\bar{c}^w)_{00} \right), \quad (7)$$

where $M_A = (\sum_w N^w m^w) - m'_A$ incorporates the conventional components of $V_{\text{int}} + T_{\text{int}}$, the total kinetic energy of all w -particles in the system is $T_{\text{int}}^w = \sum_{j=1}^{N^w} \langle (\delta p_{w,j})^2 / 2m^w \rangle$, and

$$\beta^A \equiv \frac{1}{M_A} \sum_w N^w m^w \left(\frac{2\alpha}{m^w} (\bar{a}_{\text{eff}}^w)_0 - \frac{2}{3} (\bar{c}^w)_{00} \right). \quad (8)$$

Since $(\bar{c}^w)_{00} = -(3/4)(\beta^w + \beta^{\bar{w}})$, this demonstrates that EEP tests using non-gravitationally bound systems of normal matter can constrain phenomena that would otherwise only be apparent for free antimatter particles.

We now apply Eq. (7) to evaluate the phenomenological reach of existing experiments using conventional matter. Violation of EEP is described by six independent parameters. Three for matter: β^p , β^n , and β^e ; and three for antimatter: $\beta^{\bar{p}}$, $\beta^{\bar{n}}$, and $\beta^{\bar{e}}$. For any particular EEP test comparing the effects of gravity acting on systems A and B , the observable anomaly is given by $\beta^A - \beta^B$, where β^A and β^B are defined in Eqs. (7) and (8). Since all high-precision tests of EEP are performed on charge-neutral systems, and since normal matter has a substantially similar ratio of proton to neutron content, the expression for

$\beta^A - \beta^B$ can be usefully expressed in terms of an effective neutron excess $\tilde{\Delta}_j$, effective mass defect \tilde{m}'_j , and kinetic energy components $T_{j,\text{int}}^w$ of the two systems, where

$$\tilde{\Delta}_j \equiv \frac{m^n}{m^p} \frac{m^e + m^p}{m^n} N_j^n - N_j^p, \quad (9)$$

$$\tilde{m}'_j \equiv m'_j - \frac{(m^n - m^p)(m^e + m^p)}{m^n} N_j^p, \quad (10)$$

and $j \in \{A, B\}$. The EEP-violating observable can then be written in terms of linear combinations of the free particle (β^w) and anti-particle ($\beta^{\bar{w}}$) anomalies as

$$\begin{aligned} \beta^A - \beta^B = & \frac{(m^n)^2}{(m^n)^2 + (m^e + m^p)^2} \left[\left(\frac{\tilde{\Delta}_A}{M_A} - \frac{\tilde{\Delta}_B}{M_B} \right) m^p \beta^{e+p-n} - \left(\frac{\tilde{m}'_A}{M_A} - \frac{\tilde{m}'_B}{M_B} \right) \beta^{e+p+n} \right] \\ & - \frac{1}{2} \sum_w \left(\frac{T_{A,\text{int}}^w}{M_A c^2} - \frac{T_{B,\text{int}}^w}{M_B c^2} \right) (\beta^w + \beta^{\bar{w}}), \end{aligned} \quad (11)$$

where M_A and M_B are the masses of the two test bodies, and

$$\beta^{e+p-n} \equiv \beta^{e+p} - \frac{m^e + m^p}{m^n} \beta^n \quad (12)$$

$$\beta^{e+p+n} \equiv \frac{m^e + m^p}{m^n} \beta^{e+p} + \beta^n, \quad (13)$$

in which

$$\beta^{e+p} \equiv \frac{m^e}{m^p} \beta^e + \beta^p, \quad (14)$$

after the notation of [6]. We can define a similar set of terms $\beta^{\bar{e}+\bar{p}}$, $\beta^{\bar{e}+\bar{p}-\bar{n}}$, and $\beta^{\bar{e}+\bar{p}+\bar{n}}$ for antimatter. Note that Eq. (11) has a close parallel with older studies of EEP-violation [2], since

$$\left(\frac{\tilde{m}'_B}{M_B} - \frac{\tilde{m}'_A}{M_A} \right) = \left(\frac{\tilde{A}_B}{M_B} - \frac{\tilde{A}_A}{M_A} \right) m^n, \quad (15)$$

where the effective baryon number \tilde{A}_j is given by

$$\tilde{A}_j \equiv N_j^n + \frac{m^p}{m^n} \frac{m^e + m^p}{m^n} N_j^p. \quad (16)$$

Thus the quantities $m^p \beta^{e+p-n}$ and $m^n \beta^{e+p+n}$ in the SME may be understood as parameterizing an anomalous gravitational coupling to a given particle's neutron-excess and total baryon number "charges" [2].

In our prior analysis [7], the kinetic energy of protons and neutrons bound within a given nucleus was estimated by treating the nucleons as Fermi gases confined within a square potential well. This model did not account for the nucleons' angular momentum, treated the Coulomb potential in a heuristic way by shifting the depth of the proton potential, and did not account for the nucleons' spin-orbit interaction. The latter is of particular significance,

TABLE I. Comparison between calculated bound kinetic energies (in MeV) of protons and neutrons in light nuclei, obtained from many-body Green's function Monte-Carlo (GFMC) calculations [25], and a single-particle calculation using a modified Woods-Saxon potential.

Species	GFMC		Woods-Saxon	
	T_{int}^p	T_{int}^n	T_{int}^p	T_{int}^n
${}^6\text{Li}$	77	78	64	65
${}^7\text{Li}$	88	108	67	84
${}^9\text{Be}$	124	135	95	112
${}^{10}\text{B}$	162	164	116	122
${}^{12}\text{C}$	219	219	145	153

because it can affect the occupation number of states with a given kinetic energy. Here, we improve upon that work by modeling the nucleons as single particles bound within fixed, spherically symmetric rounded square well potentials. These Woods-Saxon potentials [20] are taken to be of the form developed by Schwierz *et al.* [21]. Nuclide data is taken from Audi *et al.* [22], and isotopic abundances (for deriving the EEP-violating signal in bulk materials) from Laeter *et al.* [23]. A complete summary of our calculated kinetic energies can be found in the Supplement [24]. Better estimates of the nucleons' bound kinetic energies are available for light nuclei using Green's function Monte-Carlo (GFMC) calculations of the many-nucleon wave functions for nuclides with $A \leq 12$ [25]. The GFMC estimates of the bound kinetic energy of the constituent protons and neutrons in ${}^6\text{Li}$, ${}^7\text{Li}$, ${}^9\text{Be}$, ${}^{10}\text{B}$, and ${}^{12}\text{C}$ are summarized in Tab. I, and are compared with the corresponding predictions of our Woods-Saxon potential. Using these estimates, we can determine the contribution of the matter-sector $\beta^{e+p\pm n}$ and antimatter-sector $\beta^{\bar{e}+\bar{p}\pm\bar{n}}$ parameters to any observed violation of EEP in the motion of two (normal matter) test masses. These contributions are summarized in Fig. 1. Species with particular relevance to existing or planned tests of EEP [27–33] are explicitly labeled.

In most experiments, β^{e+p-n} is dominant, as it scales with the neutron excess. The next most accessible are the β^{e+p+n} term, which scales with the mass defect, and the antimatter term $\beta^{\bar{e}+\bar{p}-\bar{n}}$, which scales with the excess of the neutrons' kinetic energy over that of the protons, followed by $\beta^{\bar{e}+\bar{p}+\bar{n}}$. In some cases, (*e.g.* tests comparing lead and aluminium [29]) the signal from the antimatter $\beta^{\bar{e}+\bar{p}-\bar{n}}$ may actually be stronger than that from β^{e+p+n} . These terms represent four of the six degrees of freedom describing isotropic EEP violation, primarily for protons, neutrons and their antiparticles. Electronic EEP-violation is described by $\beta^{e-p} + \beta^{\bar{e}-\bar{p}} \equiv -\frac{4}{3}[(\bar{c}^e)_{00} - \frac{m^e}{m^p}(\bar{c}^p)_{00}]$, and has thus far been constrained largely by gravitational redshift tests [11–16], and tests of local Lorentz invariance [34, 35]. The sixth degree of

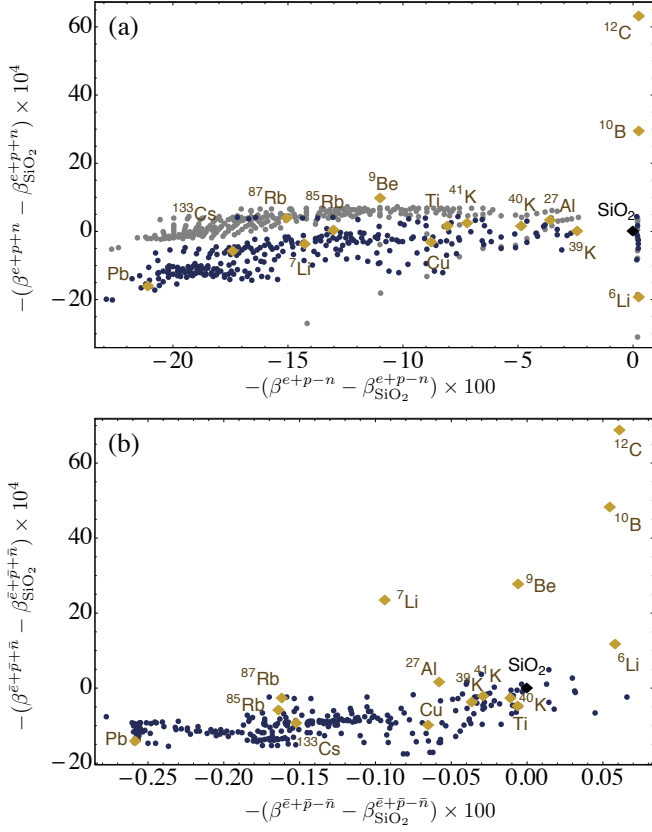


FIG. 1. Scatterplot of the contribution of $\beta^{e+p\pm n}$ and $\beta^{\bar{e}+\bar{p}\pm\bar{n}}$ parameters to observable EEP violation in normal nuclides with lifetimes in excess of 1 Gyr, when compared to SiO_2 . Tests that compare two or more widely separated species are more sensitive than tests involving neighboring isotopes. Plot (a) shows each species' relative sensitivity to matter-sector EEP-violation, and (b) depicts their sensitivities to antimatter-sector anomalies. Gray points in (a) indicate the range of sensitivities obtained without accounting for nucleons' kinetic energies. Sensitivities of ${}^6\text{Li}$, ${}^7\text{Li}$, ${}^9\text{Be}$, ${}^{10}\text{B}$, and ${}^{12}\text{C}$ are taken from GFMC calculations, all others from a Woods-Saxon model (see Supplement [24]).

freedom, $\beta^{e-p} - \beta^{\bar{e}-\bar{p}} \propto \alpha(\bar{a}_{\text{eff}}^p)_0 - \alpha(\bar{a}_{\text{eff}}^e)_0$, is only observable in tests on charged bodies [6, 18].

Using multivariate normal analysis of the results of an ensemble of EEP tests, including matter-wave [7, 9, 10], clock comparison [11–17], and torsion pendulum experiments [8], we obtain new limits on the five isotropic EEP-violating degrees of freedom that are observable in neutral systems, summarized in Tab. II. These bounds improve upon prior [7] gravitational constraints on these SME coefficients by factors of two to ten, and are also stated in terms of the five matter and anti-matter $\beta^{e+p\pm n}$, $\beta^{\bar{e}+\bar{p}\pm\bar{n}}$, and $\beta^{e-p} + \beta^{\bar{e}-\bar{p}}$ coefficients. Though the limits reported in Tab. II are necessarily model-dependent, they are stable against small variations in the estimated value of T^w/Mc^2 for the relevant nuclides, and are consistent with the limits obtained using sub-

TABLE II. Global limits ($\times 10^6$) on isotropic EEP-violation, obtained via multivariate normal analysis on the results of an ensemble of precision tests of EEP. Limits are stated in the Sun-Centered, Celestial Equatorial Frame [5], and are expressed in terms of the β^w parameters as well as the individual $(\bar{c}^w)_{TT}$ and $\alpha(\bar{a}^w)_T$, with $(\bar{a}^{e+p})_T \equiv (\bar{a}^e)_T + (\bar{a}^p)_T$. Also shown is the limit on the 1σ volume β^{II} of five-dimensional parameter space consistent with experiment.

$(\beta^{e-p} + \beta^{\bar{e}-\bar{p}})$	0.019 ± 0.037	$(\bar{c}^e)_{TT}$	-0.014 ± 0.028
β^{e+p-n}	-0.013 ± 0.021	$(\bar{c}^n)_{TT}$	1.1 ± 1.4
β^{e+p+n}	2.4 ± 3.9	$(\bar{c}^p)_{TT}$	0.24 ± 0.30
$\beta^{\bar{e}+\bar{p}-\bar{n}}$	1.1 ± 1.8	$\alpha(\bar{a}^n)_T$	0.51 ± 0.64
$\beta^{\bar{e}+\bar{p}+\bar{n}}$	-4.1 ± 6.7	$\alpha(\bar{a}^{e+p})_T$	0.22 ± 0.28

stantially different nuclear models [26].

Despite the fact that torsion pendulum tests [8] set limits on specific combinations of β parameters at the level of 10^{-12} (having constrained $\Delta g/g$ to the level of 10^{-14}), the best bounds reported in Tab. II are at the level of 10^{-8} . This apparent discrepancy is due to the fact that such tests do not span the full parameter space considered here. Thus the limits on the individual β 's summarized in Tab. II are strongly correlated with one another. Analysis of these correlations reveals that some combinations of the β 's are indeed constrained at the level of 10^{-9} , 10^{-11} and 10^{-12} , thanks to matter-wave interferometer and torsion pendulum results. Unfortunately, the specific combinations of β 's subject to these constraints are sensitive to small errors in our estimates of the nuclides' bound kinetic energy, due to disparities between the precision of torsion pendulums and of other EEP tests. Formal limits on EEP-violation at the level of an effective field theory like the SME must therefore await the development of more reliable nuclear models [26] or the results of additional high precision EEP test presently in development, using matter-waves [31–33], clocks [28] or macroscopic masses [29, 30].

We have demonstrated that EEP tests on non-gravitationally bound systems of normal particles can set indirect constraints on EEP-violation in antimatter, thanks to the interaction between the EEP-violating terms and the system's bound kinetic energy. We have explicitly derived the link between anomalous gravitational redshifts and violations of the weak equivalence principle. This occurs whenever EEP is violated by introducing a particle-specific metric. In the context of the SME, accounting for these interactions results in significantly improved constraints on EEP-violation in the standard model lagrangian, for both matter and antimatter. The precision of these bounds is limited by that of existing nuclear models, and uneven experimental coverage of EEP-violating parameter space. New EEP tests with precision comparable to that of existing torsion pendulum experiments [28–33] may substantially eliminate

this model-dependent limitation. Better nuclear modeling could also improve limits on EEP violation in the SME by up to eight orders of magnitude, the pursuit of which will be the subject of future work.

We thank Brian Estey, Paul Hamilton, Alan Kostelecký and Jay Tasson for stimulating discussions. We also thank W. Nazarewicz and N. Birge for providing us with independent estimates of the bound kinetic energy of nucleons in a range of atomic species.

* hohensee@berkeley.edu

- [1] C.W. Misner, K.S. Thorne, and J.A. Wheeler, *Gravitation* (Freeman, San Francisco, 1970).
- [2] T. Damour, *Class. Quant. Grav.* **13**, A33 (1996).
- [3] V.A. Kostelecký and S. Samuel, *Phys. Rev. D* **39**, 683 (1989).
- [4] D. Colladay and V.A. Kostelecký, *Phys. Rev. D* **55**, 6760 (1997); *Phys. Rev. D* **58**, 116002 (1998).
- [5] N. Russell and V.A. Kostelecký, *Rev. Mod. Phys.* **83**, 11 (2011); arXiv:0801.0287 [hep-ph] (2012).
- [6] V.A. Kostelecký and J.D. Tasson, *Phys. Rev. D* **83**, 016013 (2011).
- [7] M.A. Hohensee, S. Chu, A. Peters, and H. Müller, *Phys. Rev. Lett.* **106**, 151102 (2011).
- [8] S. Schlamminger, K.-Y. Choi, T.A. Wagner, J.H. Gundlach, and E.G. Adelberger, *Phys. Rev. Lett.* **100**, 041101 (2008); J.H. Gundlach, S. Schlamminger, and T.A. Wagner, *Space Sci. Rev.* **148**, 201 (2009); Y. Su *et al.*, *Phys. Rev. D* **50**, 3614 (1994).
- [9] H. Müller, A. Peters, and S. Chu, *Nature*, **463**, 926 (2010); **467**, E2 (2010).
- [10] N. Poli *et al.*, *Phys. Rev. Lett.* **106**, 038501 (2011); P. Cladé *et al.*, *Europhys. Lett.* **71**, 730 (2005); S. Merlet *et al.*, *Metrologia* **47**, L9 (2010).
- [11] R.F.C. Vessot *et al.*, *Phys. Rev. Lett.* **45**, 2081 (1980).
- [12] R.V. Pound and G.A. Rebka Jr., *Phys. Rev. Lett.* **4**, 337 (1960); R.V. Pound and J.L. Snider, *Phys. Rev. Lett.* **13**, 539 (1964); *Phys. Rev.* **140**, B788 (1965).
- [13] N. Ashby *et al.*, *Phys. Rev. Lett.* **98**, 070802 (2007).
- [14] S. Blatt *et al.*, *Phys. Rev. Lett.* **100**, 140801 (2008).
- [15] T. M. Fortier *et al.*, *Phys. Rev. Lett.* **98**, 070801 (2007).
- [16] M.A. Hohensee, N. Leefler, D. Budker, C. Harabati, V.A. Dzuba, and V.V. Flambaum, *Phys. Rev. Lett.* **111**, 050401 (2013).
- [17] V.A. Kostelecký and J.D. Tasson, *Phys. Rev. Lett.* **102**, 010402 (2009).
- [18] M.A. Hohensee and H. Müller, *J. Mod. Opt.* **58**, 2021 (2011).
- [19] C.M. Will, *Liv. Rev. Relativity* **9**, 3 (2006).
- [20] R.D. Woods and D.S. Saxon, *Phys. Rev.* **95**, 577 (1954).
- [21] N. Schwierz, I. Wiedenhover and A. Volya, arXiv:0709.3525 [nucl-th] (2007).
- [22] G. Audi, A.H. Wapstra and C. Thibault, *Nuclear Physics A* **729**, 337 (2003).
- [23] J.R. De Laeter, *et al.*, *Pure Appl. Chem.* **75**, 683 (2003).
- [24] See the Supplemental Material for the full form of the single-particle Hamiltonian used to estimate the bound kinetic energies of protons and neutrons within an atomic nucleus, and for a table of calculated proton and neutron kinetic energies.
- [25] S.C. Pieper and R.B. Wiringa, *Annu. Rev. Nucl. Part. Sci.* **51**, 53 (2001).
- [26] N. Birge, *et al.*, to be published.
- [27] S. Dimopoulos, P.W. Graham, J.M. Hogan, and M.A. Kasevich, *Phys. Rev. D* **78**, 042003 (2008); *Phys. Rev. Lett.* **98**, 111102 (2007).
- [28] J. Páramos and G. Hechenblaikner, arXiv:1210.7333 (2012).
- [29] R.D. Reasenberg *et al.*, *Class. Quant. Grav.* **28**, 094014 (2011); R.D. Reasenberg, B.R. Patla, J.D. Phillips, and R. Thapa, arXiv:1206.0028 (2012).
- [30] A.M. Nobili *et al.*, *Class. Quant. Grav.* **29**, 184011 (2012).
- [31] H. Müntinga *et al.*, arXiv:1301.5883 (2013).
- [32] J.M. Hogan, D.M.S. Johnson, and M.A. Kasevich, *Proc. Int. Sch. Phys. “Enrico Fermi”*, **168**, 411 (2009).
- [33] P. Hamilton, T. Barter, G. Kim, B. Mukherjee, and H. Müller, *Bull. Am. Phys. Soc.* **57**, T5.00004 (2012).
- [34] V.A. Kostelecký and C.D. Lane, *Phys. Rev. D* **60**, 116010 (1999).
- [35] M.A. Hohensee, R. Lehnert, D.F. Phillips, and R.L. Walsworth, *Phys. Rev. Lett.* **102**, 170402 (2009); *Phys. Rev. D* **80**, 036010 (2009); B. Altschul, *Phys. Rev. D* **80**, 091901(R) (2009); J.-P. Bocquet *et al.* *Phys. Rev. Lett.* **104**, 241601 (2010);

SUPPLEMENTAL MATERIAL

In a previous analysis [7], we estimated the kinetic energy of the protons and neutrons bound within a given nucleus by treating the nucleons as fermi gases confined to a square potential well. Here we improve upon that work using a shell model calculation. The nucleus is modeled as a pair of rounded, spherically symmetric square well, or Woods-Saxon, potentials which separately confine its constituent protons and neutrons. Our potential is that of [21], although we do not work with relative coordinates, and so do not use the reduced particle mass in our Hamiltonian. For a nucleon of mass m^w in a nucleus with mass number $A = Z + N$, made up of Z protons and N neutrons, our model Hamiltonian is [21]

$$H = \frac{p^2}{2m^w} + V_0 \left(1 - \frac{4\kappa}{A} \langle \mathbf{t} \cdot \mathbf{T}' \rangle \right) f(r, R, a) + V_c(r, R) + \frac{1}{2(m^w)^2 r} \left(\frac{\partial}{\partial r} \tilde{V} f(r, R_{SO}, a) \right) \mathbf{L} \cdot \mathbf{S}, \quad (17)$$

The Woods-Saxon potential is given by

$$f(r, R, a) = \frac{1}{1 + e^{(r-R)/a}}, \quad (18)$$

and $V_0 = -52.06$ MeV, $\tilde{V} = 24.1V_0$, $R = 1.26A^{1/3}$ fm, $R_{SO} = 1.16A^{1/3}$ fm, $a = 0.662$ fm. The vectors \mathbf{t} and \mathbf{T}' are the isospin of the nucleon and of the nucleus less that nucleon, respectively, and as in [21], are taken to be

such that

$$-4\langle \mathbf{t} \cdot \mathbf{T}' \rangle = \begin{cases} 3, & N = Z \\ \pm (N - Z + 1) + 2, & N > Z \\ \pm (N - Z - 1) + 2, & N < Z, \end{cases} \quad (19)$$

with $\kappa = 0.639$. The Coulomb potential $V_c(r)$ applies only to protons, and is given by

$$V_c(r, R) = (Z - 1)e^2 \begin{cases} \frac{3R^2 - r^2}{2R^3}, & r \leq R \\ \frac{1}{r}, & r > R. \end{cases} \quad (20)$$

We solve for the eigenstates of this Hamiltonian numer-

ically, and assign the protons and neutrons respectively to the Z and N lowest-lying energy states. We then evaluate and sum the expectation value of the kinetic energy operator $\langle p^2/2m \rangle$ for each occupied state, to obtain the kinetic energy correction term of Eq. (7). The total estimated nucleon kinetic energies for all stable, and many long-lived nuclides are shown in Tables III and IV. The accuracy of these estimates is not guaranteed, as experimental measurements of the nucleons' bound kinetic energy are unavailable, and these results are derived from models that have been optimized for the solution of other problems [21]. Nevertheless, they do yield limits on the β coefficients (see Tab. II) that are consistent with those derived using other nuclear models [26], and exhibit similar trends.

TABLE III. Estimated bound kinetic energies (in MeV) of protons (T_{int}^p) and neutrons (T_{int}^n) in stable nuclides.

Species	T_{int}^p	T_{int}^n	Species	T_{int}^p	T_{int}^n	Species	T_{int}^p	T_{int}^n	Species	T_{int}^p	T_{int}^n	Species	T_{int}^p	T_{int}^n
⁶ Li	64	65	⁵⁴ Cr	559	659	⁹⁴ Mo	831	1079	¹³⁰ Ba	1211	1636	¹⁶⁹ Tm	1405	2233
⁷ Li	67	84	⁵⁴ Fe	590	662	⁹⁵ Mo	886	1097	¹³¹ Xe	1173	1692	¹⁷⁰ Er	1383	2266
⁹ Be	95	112	⁵⁵ Mn	576	667	⁹⁶ Mo	903	1114	¹³² Xe	1171	1712	¹⁷⁰ Yb	1424	2157
¹⁰ B	116	122	⁵⁶ Fe	574	674	⁹⁶ Ru	869	1088	¹³² Ba	1208	1678	¹⁷¹ Yb	1422	2188
¹¹ B	124	143	⁵⁷ Fe	575	680	⁹⁷ Mo	903	1131	¹³³ Cs	1189	1716	¹⁷² Yb	1421	2311
¹² C	145	153	⁵⁸ Fe	576	686	⁹⁸ Mo	903	1148	¹³⁴ Xe	1168	1753	¹⁷³ Yb	1419	2249
¹³ C	154	165	⁵⁸ Ni	608	685	⁹⁸ Ru	868	1124	¹³⁴ Ba	1206	1719	¹⁷⁴ Yb	1417	2279
¹⁴ N	165	173	⁵⁹ Co	593	692	⁹⁹ Ru	924	1141	¹³⁵ Ba	1204	1739	¹⁷⁵ Lu	1436	2295
¹⁵ N	172	185	⁶⁰ Ni	610	697	¹⁰⁰ Ru	958	1159	¹³⁶ Xe	1165	1793	¹⁷⁶ Yb	1413	2340
¹⁶ O	183	191	⁶¹ Ni	610	721	¹⁰¹ Ru	958	1197	¹³⁶ Ba	1203	1760	¹⁷⁶ Hf	1454	2308
¹⁷ O	188	211	⁶² Ni	611	745	¹⁰² Ru	958	1217	¹³⁶ Ce	1239	1724	¹⁷⁷ Hf	1452	2338
¹⁸ O	192	215	⁶³ Cu	616	751	¹⁰² Pd	904	1224	¹³⁷ Ba	1201	1780	¹⁷⁸ Hf	1451	2368
¹⁹ O	211	235	⁶⁴ Ni	610	792	¹⁰³ Rh	985	1268	¹³⁸ Ba	1200	1799	¹⁷⁹ Hf	1449	2398
²⁰ Ne	229	240	⁶⁴ Zn	622	776	¹⁰⁴ Ru	957	1254	¹³⁸ Ce	1236	1765	¹⁸⁰ Hf	1447	2428
²¹ Ne	233	258	⁶⁵ Cu	616	799	¹⁰⁴ Pd	1011	1279	¹³⁹ La	1217	1802	¹⁸⁰ W	1487	2390
²² Ne	236	264	⁶⁶ Zn	622	825	¹⁰⁵ Pd	1011	1306	¹⁴⁰ Ce	1233	1805	¹⁸¹ Ta	1465	2439
²³ Na	254	289	⁶⁷ Zn	622	849	¹⁰⁶ Pd	1011	1333	¹⁴¹ Pr	1241	1807	¹⁸² W	1483	2449
²⁴ Mg	271	300	⁶⁸ Zn	622	872	¹⁰⁶ Cd	996	1295	¹⁴² Ce	1230	1840	¹⁸³ W	1481	2479
²⁵ Mg	274	321	⁶⁹ Ga	628	878	¹⁰⁷ Ag	1038	1342	¹⁴² Nd	1249	1808	¹⁸⁴ W	1479	2508
²⁶ Mg	276	319	⁷⁰ Zn	638	882	¹⁰⁸ Pd	1010	1386	¹⁴³ Nd	1248	1826	¹⁸⁴ Os	1520	2517
²⁷ Al	292	352	⁷⁰ Ge	634	883	¹⁰⁸ Cd	1064	1349	¹⁴⁴ Sm	1265	1811	¹⁸⁵ Re	1497	2550
²⁸ Si	308	361	⁷¹ Ga	627	888	¹⁰⁹ Ag	1037	1395	¹⁴⁵ Nd	1245	1862	¹⁸⁶ W	1475	2648
²⁹ Si	310	361	⁷² Ge	633	894	¹¹⁰ Pd	1009	1438	¹⁴⁶ Nd	1243	1880	¹⁸⁷ Os	1513	2581
³⁰ Si	349	346	⁷³ Ge	668	920	¹¹⁰ Cd	1063	1402	¹⁴⁸ Nd	1258	1915	¹⁸⁸ Os	1511	2603
³¹ P	312	369	⁷⁴ Ge	668	947	¹¹¹ Cd	1063	1429	¹⁴⁹ Sm	1257	1885	¹⁸⁹ Os	1509	2624
³² S	312	375	⁷⁴ Se	667	902	¹¹² Cd	1062	1455	¹⁵⁰ Sm	1256	1903	¹⁹⁰ Os	1507	2645
³³ S	353	396	⁷⁵ As	685	952	¹¹² Sn	1115	1414	¹⁵¹ Eu	1264	1905	¹⁹¹ Ir	1515	2653
³⁴ S	359	402	⁷⁶ Se	666	957	¹¹³ In	1089	1461	¹⁵² Sm	1290	1938	¹⁹² Os	1533	2663
³⁵ Cl	373	424	⁷⁷ Se	701	984	¹¹⁴ Cd	1061	1450	¹⁵³ Eu	1260	1941	¹⁹² Pt	1522	2661
³⁶ S	368	441	⁷⁸ Se	701	1011	¹¹⁴ Sn	1114	1467	¹⁵⁴ Sm	1287	1979	¹⁹³ Ir	1519	2671
³⁶ Ar	386	430	⁷⁸ Kr	699	965	¹¹⁵ Sn	1114	1465	¹⁵⁴ Gd	1268	1926	¹⁹⁴ Pt	1535	2679
³⁷ Cl	390	451	⁷⁹ Br	717	1016	¹¹⁶ Sn	1113	1463	¹⁵⁵ Gd	1267	1946	¹⁹⁵ Pt	1532	2688
³⁸ Ar	397	460	⁸⁰ Se	701	1064	¹¹⁷ Sn	1113	1478	¹⁵⁶ Gd	1321	1966	¹⁹⁶ Pt	1543	2697
³⁹ K	410	481	⁸⁰ Kr	733	1020	¹¹⁸ Sn	1112	1494	¹⁵⁶ Dy	1309	1929	¹⁹⁶ Hg	1533	2692
⁴⁰ Ar	419	501	⁸¹ Br	717	1069	¹¹⁹ Sn	1111	1509	¹⁵⁷ Gd	1319	1986	¹⁹⁷ Au	1546	2704
⁴⁰ Ca	423	486	⁸² Kr	733	1074	¹²⁰ Sn	1110	1524	¹⁵⁸ Gd	1318	2006	¹⁹⁸ Pt	1539	2716
⁴¹ K	440	509	⁸³ Kr	772	1101	¹²⁰ Te	1147	1504	¹⁵⁸ Dy	1306	1970	¹⁹⁸ Hg	1529	2711
⁴² Ca	460	515	⁸⁴ Kr	810	1127	¹²¹ Sb	1128	1530	¹⁵⁹ Tb	1338	2008	¹⁹⁹ Hg	1560	2720
⁴³ Ca	466	535	⁸⁴ Sr	782	1082	¹²² Sn	1108	1568	¹⁶⁰ Gd	1315	2046	²⁰⁰ Hg	1558	2729
⁴⁴ Ca	470	555	⁸⁵ Rb	777	1132	¹²² Te	1146	1535	¹⁶⁰ Dy	1357	2010	²⁰¹ Hg	1551	2738
⁴⁵ Sc	489	560	⁸⁶ Kr	809	1179	¹²³ Sb	1126	1573	¹⁶¹ Dy	1356	2029	²⁰² Hg	1549	2747
⁴⁶ Ca	476	593	⁸⁶ Sr	782	1136	¹²⁴ Sn	1106	1610	¹⁶² Dy	1354	2049	²⁰³ Tl	1556	2753
⁴⁶ Ti	507	520	⁸⁷ Sr	781	1163	¹²⁴ Te	1144	1579	¹⁶² Er	1343	2059	²⁰⁴ Hg	1590	2765
⁴⁷ Ti	511	548	⁸⁸ Sr	838	1189	¹²⁴ Xe	1181	1544	¹⁶³ Dy	1353	2069	²⁰⁴ Pb	1551	2758
⁴⁸ Ti	514	575	⁸⁹ Y	786	1193	¹²⁵ Te	1143	1600	¹⁶⁴ Dy	1351	2088	²⁰⁵ Tl	1552	2771
⁴⁹ Ti	517	602	⁹⁰ Zr	792	1197	¹²⁶ Te	1142	1621	¹⁶⁴ Er	1393	2113	²⁰⁶ Pb	1559	2777
⁵⁰ Ti	519	628	⁹¹ Zr	791	1206	¹²⁶ Xe	1179	1587	¹⁶⁵ Ho	1370	2154	²⁰⁷ Pb	1557	2786
⁵⁰ Cr	550	593	⁹² Zr	848	1214	¹²⁷ I	1159	1626	¹⁶⁶ Er	1390	2167	²⁰⁸ Pb	1555	2795
⁵¹ V	537	638	⁹² Mo	831	1045	¹²⁸ Xe	1177	1630	¹⁶⁷ Er	1388	2193			
⁵² Cr	555	648	⁹³ Nb	867	1218	¹²⁹ Xe	1175	1651	¹⁶⁸ Er	1386	2220			
⁵³ Cr	557	653	⁹⁴ Zr	847	1231	¹³⁰ Xe	1174	1671	¹⁶⁸ Yb	1428	2119			

TABLE IV. Estimated bound kinetic energies (in MeV) of protons (T_{int}^p) and neutrons (T_{int}^n) in long-lived nuclides.

Species	T_{int}^p	T_{int}^n	Species	T_{int}^p	T_{int}^n	Species	T_{int}^p	T_{int}^n	Species	T_{int}^p	T_{int}^n	Species	T_{int}^p	T_{int}^n
⁴⁰ K	435	488	¹⁹⁰ Pt	1526	2619	⁸² Se	780	1115	²⁰⁹ Bi	1573	2783	¹⁸⁶ Os	1515	2560
⁸⁷ Rb	824	1184	²³² Th	1761	3048	⁹⁶ Zr	846	1249	⁵⁰ V	535	612	¹¹⁵ In	1087	1457
¹³⁸ La	1218	1782	²³⁸ U	1804	3161	¹⁰⁰ Mo	902	1186	¹¹³ Cd	1062	1453	¹²³ Te	1145	1557
¹⁴⁷ Sm	1260	1848	¹²⁸ Te	1139	1663	¹¹⁶ Cd	1060	1480	¹⁴⁴ Nd	1246	1844	¹⁵² Gd	1271	1889
¹⁷⁶ Lu	1434	2325	⁷⁶ Ge	668	999	¹³⁰ Te	1136	1704	¹⁴⁸ Sm	1259	1867			
¹⁸⁷ Re	1493	2593	⁴⁸ Ca	480	629	¹⁵⁰ Nd	1255	1950	¹⁷⁴ Hf	1458	2247			